Oudbashi *et al. Herit Sci* (2021) 9:83
https://doi.org/10.1186/s40494-021-00557-6

Heritage Science

RESEARCH ARTICLE Open Access

# The pottery production from the Deh Dumen Bronze Age graveyard (South-Western Iran): a chemical, mineralogical and physical study

Omid Oudbashi[1,2*], Reza Naseri[3], Giuseppe Cultrone[4], Isabel Egartner[5] and Anna Arizzi[4]

**Abstract**

A collection of pottery vessels uncovered during the first season of excavations in the Deh Dumen Bronze Age graveyard (the second half of the third millennium BC) located in south-western Iran were studied by using chemical, mineralogical and physical techniques, with the aim to identify the pottery manufacturing process in this region. The site is located in a region of the Zagros fold and thrust belt that includes carbonate rocks and alluvial deposits. The pottery vessels found in the site present two different fabric types in their fresh surface: bright yellowish hue fabric (TYPE-1) and sandwich-like or black core fabric (TYPE-2) showing presumably different production techniques or workshops. Twenty-four samples from pottery sherds were selected and analysed by X-ray fluorescence (XRF), powder X-ray diffraction (XRD), polarized light microscopy (PLM), and field emission scanning electron microscopy (FESEM). Hydric tests were also performed. Samples were different according to their chemistry having distinguished calcium-rich and calcium-poor ceramics. $Al_2O_3$ and $Fe_2O_3$ were detected as the other main components of samples besides $SiO_2$ and CaO. The mineralogical and textural characterisation revealed a fine-grained clayey matrix with quartz and feldspar grains in TYPE-1 potteries and large and small calcitic and clayey lumps inclusions in TYPE-2 potteries. Imprints of straw or other plants can be responsible for the higher porosity of some of the potteries. It was found that most of the potteries from the Deh Dumen graveyard were produced by means of a local and traditional pottery manufacturing technique, whilst others may have been produced in different places and transported to the graveyard as ritual offerings.

**Keywords:** Bronze Age, Deh Dumen graveyard, Pottery production, Sandwich-like structure, Temper

## Introduction

The history of ceramic technology in the Iranian Plateau dates back to ca. 10,000 years ago, showing the importance of this craft in the technological development of this region during the prehistoric era [1, 2]. The early samples of potteries (sherds or wares, that seem more hand-made, chaff-tempered) are found in Neolithic sites as those in Deh Luran and Khuzestan lowland regions. They are located in western and south-western Iran, in early villages within the Zagros Mountain, some in Neolithic caves of northern Iran and other in Neolithic sites round the Plateau [3–8]. The technology was improved further during Chalcolithic (ca. 5500 – 3000 BC), Bronze Age (ca. 3000 – 1500 BC) and Iron Age (ca.1500 – 550 BC) by the emergence of different types of ceramic products such as wheel-made potteries, painted potteries, bulk red, yellow and grey potteries (wares) [1]. On the other hand, the ceramic technology was extended with the production of other types of ceramics, such as simple

*Correspondence: o.oudbashi@aui.ac.ir
[1] Department of Conservation of Cultural and Historical Properties, Art University of Isfahan, Isfahan, Iran
Full list of author information is available at the end of the article

and glazed bricks as well as decorative sculptural ceramic objects and decorative pottery vessels with specific forms such as rythons and human and animal figurines [9–13].

Archaeometric studies carried out in last decades on the pottery production in prehistoric Iran, have revealed different aspects of craftsmen expertise in Iranian highlands and lowlands from late Neolithic to the Iron Age. For example, thermal analysis of pottery sherds from the Neolithic site of Ganj Dareh (Western Iran) showed that those ceramics were fired probably in open fires and under poor control of firing conditions [14]. Studies of vessels from late Neolithic and Chalcolithic sites such as Sialk (central Iran) [15], Rahmatabad (south-western Iran) [16], various archaeological sites from Fars (south-central Iran) [17], Tehran Plain (north-central Iran) [18] and from Tappeh Zagheh in Qazvin Plain [19] show relatively similar compositions and homogeneous microstructures as well as significantly high firing temperatures. Furthermore, researches carried out on potteries from later periods such as those from Tappeh Yahya (north-central Iran) [20, 21], Tol-e Kamin and Malyan (south-central Iran) [22, 23], Sistan region and Shahr-i Sokhta (eastern Iran) [24–26], Godin Tepe and Kolyaei plain (western Iran) [27, 28], the ceramics from the middle Elamite sites (second millennium BC) of Haft Tappeh and Chogha Zanbil [29, 30], as well as Middle Chalcolithic ceramics from Chaharmahal-Bakhtiari province (5th -4th millennium BC) [31] show the use of local raw materials and the preservation of traditional ceramic production, even though evidences of ceramic trades are also visible. These studies revealed some interesting aspects of pottery production in prehistoric Iran, regarding for example the choice of raw materials, the additives and the conditions of the firing process.

The Deh Dumen graveyard is an important Iranian archaeological site due to its cultural and trade relationship between western and eastern regions of the Iranian Plateau as evidenced by the presence of objects that are similar to those found in other sites [32]. The archaeological studies revealed that the Deh Dumen grave goods (such as potteries and metalworks) show similarities with objects excavated from some western (Luristan), south-western (Susa) and eastern (Shahdad) Iranian Bronze Age sites (third millennium BC). This suggests that this site may have been a connecting point between east and west during the Bronze Age. Despite dating of the materials from the site is not available, comparative studies with the sites mentioned above showed that this place was used as a graveyard since the Bronze Age (ca. 3000 − 1500 BC) by people who came from different regions in Iran [32–34] (Fig. 1a). Notwithstanding, little is still known about different aspects of the life in this area of the Iranian Plateau during the Bronze Age.

Knowing that the archaeometric study of different materials, potteries in particular, can help to find evidences of ancient settlements in a specific time and place, chemical, mineralogical and textural analyses as well as physical tests were carried out on a pottery sherd collection from the Deh Dumen graveyard. This multi-analytical approach was chosen to know the technology of the pottery production in south-western Iran during the third millennium BC. More specifically, this study will also allow to investigate the reasons for the differences in the characteristics of the studied ceramics.

## Archaeological and geological background

The ancient graveyard of Deh Dumen is located in the south-western Iran, about 70 km north-west of the city of Yasuj, the capital of the Kohgiluyeh and Boyer-Ahmad province (34° 46′ 84″ N, 51° 02′ 99″ E), partially encircling the Zagros fold and thrust belt chain. This long mountain chain forms a barrier between the Iranian Plateau and the Mesopotamian lowlands (Iraq), and at the same time constitutes a corridor for a southward distribution of northern faunal elements [35]. The archaeological site is placed in the Khersan river valley beside the western side of the river. The main geological formation of the region is the carbonate Asmari Formation of Oligocene–Miocene age, known as a major hydrocarbon reservoir in south-western Iran (Figs. 1b and 2a) [36, 37]. Asmari Formation shows a high anticline in the Boyer-Ahmad and Dena Counties (regions in Kohgiluyeh and Boyer-Ahmad province) leading to the construction of deep valleys and extensive plains between high rock mountains. These valleys are covered with alluvial deposits from calcareous soils [38]. According to literature, the soil of the Kohgiluyeh and Boyer-Ahmad province and the river beds of the region are characterized by high-carbonates content with variable amounts of clay minerals such as illite ($(K,H_3O)(Al,Mg,Fe)_2(Si,Al)_4O_{10}[(OH)_2,(H_2O)]$), chlorite ($(Mg,Fe)_3(Si,Al)_4O_{10}(OH)_2\cdot(Mg,Fe)_3(OH)_6$), vermiculite ($(Mg,Fe^{++},Al)_3(Al,Si)_4O_{10}(OH)_2\cdot4(H_2O)$), palygorskite ($(Mg,Al)_2Si_4O_{10}(OH)\cdot4(H_2O)$) and smectite group minerals [39, 40]. However, it is not known if this high content of carbonates is due to the presence of fossils and microfossils, as only chemical and mineralogical but no textural investigations have been carried out on the soil so far [41, 42]. The limestone outcrops in the Deh Dumen and Khersan river region belonging to the Asmari Formation, instead, do contain various types of fossils (shells of bivalves mainly) [43, 44].

Archaeological excavations in the graveyard of Deh Dumen have been undertaken in three campaigns from 2013 to 2019 [33]. These led to discover many large graves built with stones, including two specific types of prehistoric graves: one with a smooth and flat roof

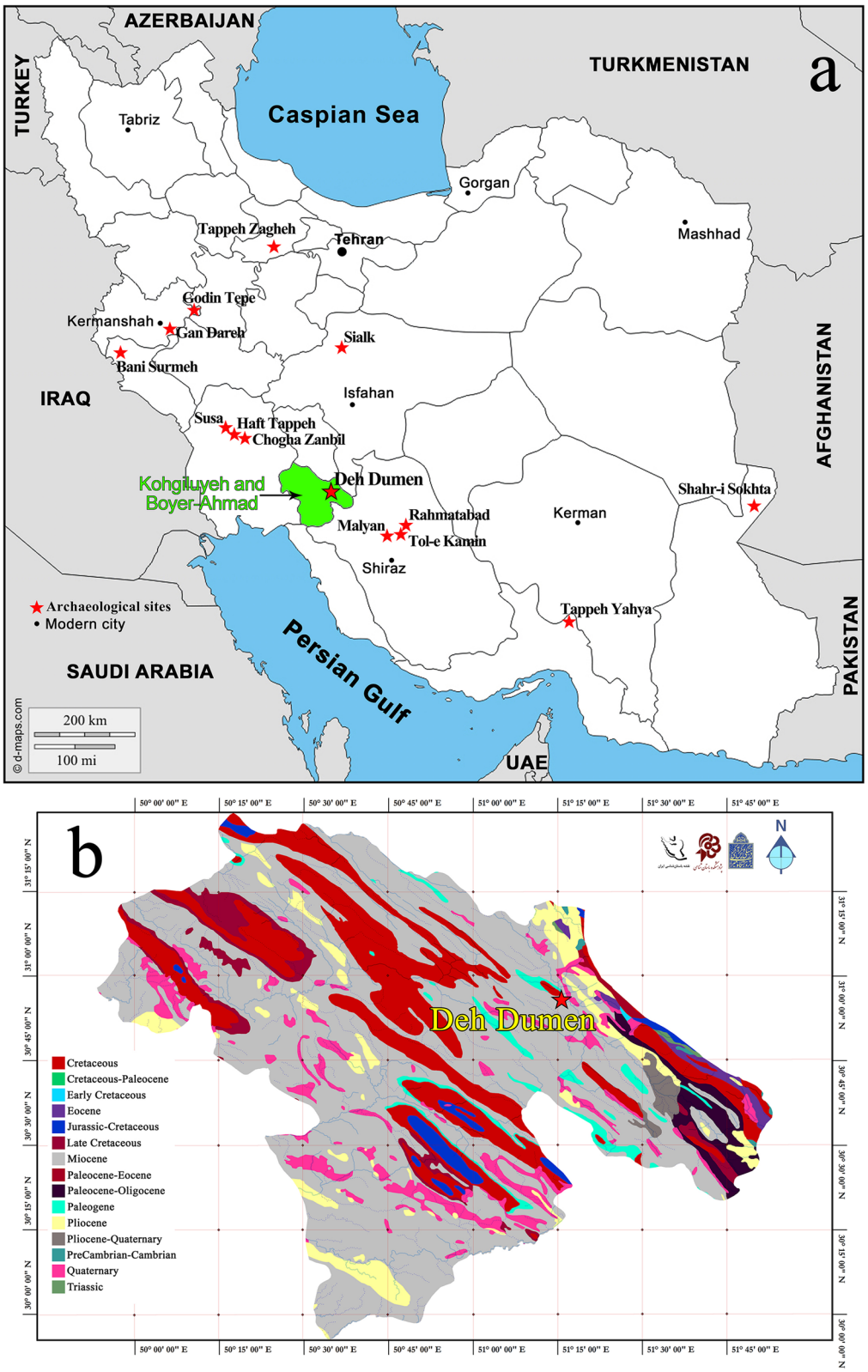


**Fig. 1** **a** Map of Iran and location of the Deh Dumen graveyard in south-western Iran and other archaeological sites mentioned in the text; **b** Geological map of Kohgiluyeh and Boyer-Ahmad province showing the main formations and location of Deh Dumen in Miocene formation of Asmari in eastern part of province (Courtesy: RICHT-ICAR Archaeological Maps Archive)

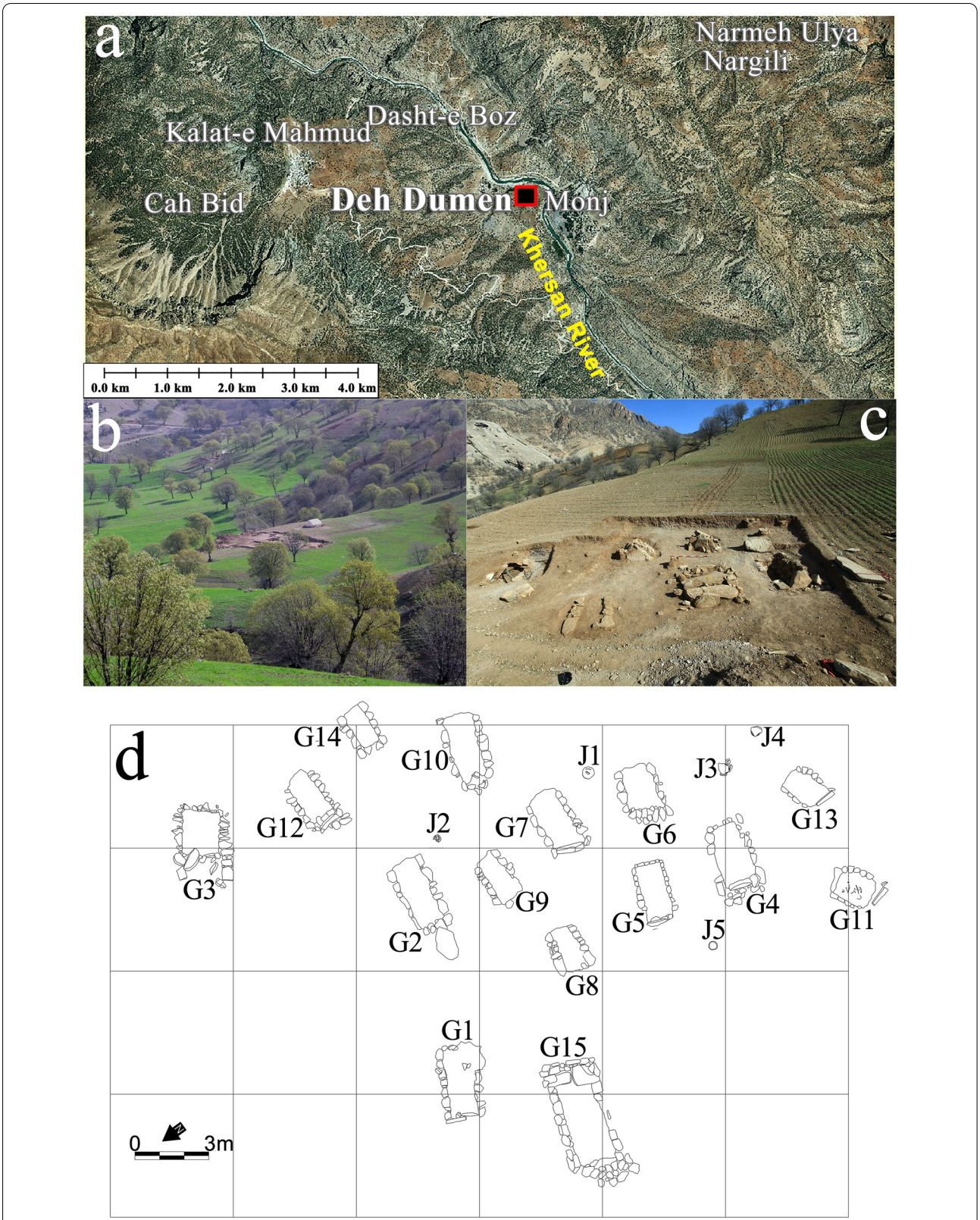


**Fig. 2** **a** Location of Deh Dumen archaeological graveyard at the southern side of the Khersan river; **b** a view from the trenches of first season excavation in Deh Dumen; **c** a closer view from trenches and graves excavated in first season; **d** plan of the area excavated in the first season in 2013 showing the graves discovered during the excavation

(box-shaped graves) and the other with a herringbone (or peaked) roof (mound graves) (Fig. 2b, c). Some burial jars were found among the stone graves (Fig. 2d) and many objects were placed close to skeletons as grave goods. They included different types of pottery such as simple and decorated vessels, different metallic objects such as vessels and weapons, as well as stone vessels and arrowheads [32, 33].

After comparing grave goods and grave constructions with similar graveyards and objects from other parts of the Iranian Plateau, it appears that the graveyard of Deh Dumen showed similarities with those belonging to the second half of the third millennium BC, despite some graves excavated during the second excavation campaign date back to second millennium BC [32–34]. For example, some of the potteries and metal vessels show stylistic similarities to the objects found in other archaeological sites of the Bronze Age located in western, south-western and eastern Iran (e.g. the graveyard of Bani Surmeh in Pusht-i Kuh Luristan; the third millennium BC level of Susa (level D) in Susiana plain; the Kerman and Sistan regions) [32].

## Materials and methods

### Archaeological ceramics studied

Among the objects discovered within the graves of Deh Dumen, many Bronze Age potteries were found, such as large jars, small handled vessels and painted potteries with very simple motifs and patterns [32]. Most of the grave potteries have a yellow (buff) and red to brown and black slipped fabric, including jars and vessels with impressed decorative bands on the body and base, as well as jars with parallel grooved and jagged decorations on the body. To investigate the crafting process of these potteries, chemical, mineralogical, textural and physical analyses were carried out on twenty-four objects. All samples were collected during the first season of excavations in the Deh Dumen graveyard, undertaken in 2013, in which 15 graves and some burial jars were excavated in the site (Fig. 2d).

Twenty-four pottery sherds from broken vases were selected for this study. Despite the limited number of samples, they are representative of the variety of potteries, which can be classified in two different groups on the basis of a first macroscopic observation (Fig. 3):

- TYPE 1: eight pottery sherd samples showing a bright yellowish hue fabric and an almost uniform and fine grain texture in the broken section.
- TYPE 2: sixteen pottery sherd samples showing a coarse grain texture with an orange-red surface layer and a black core (sandwich-like).

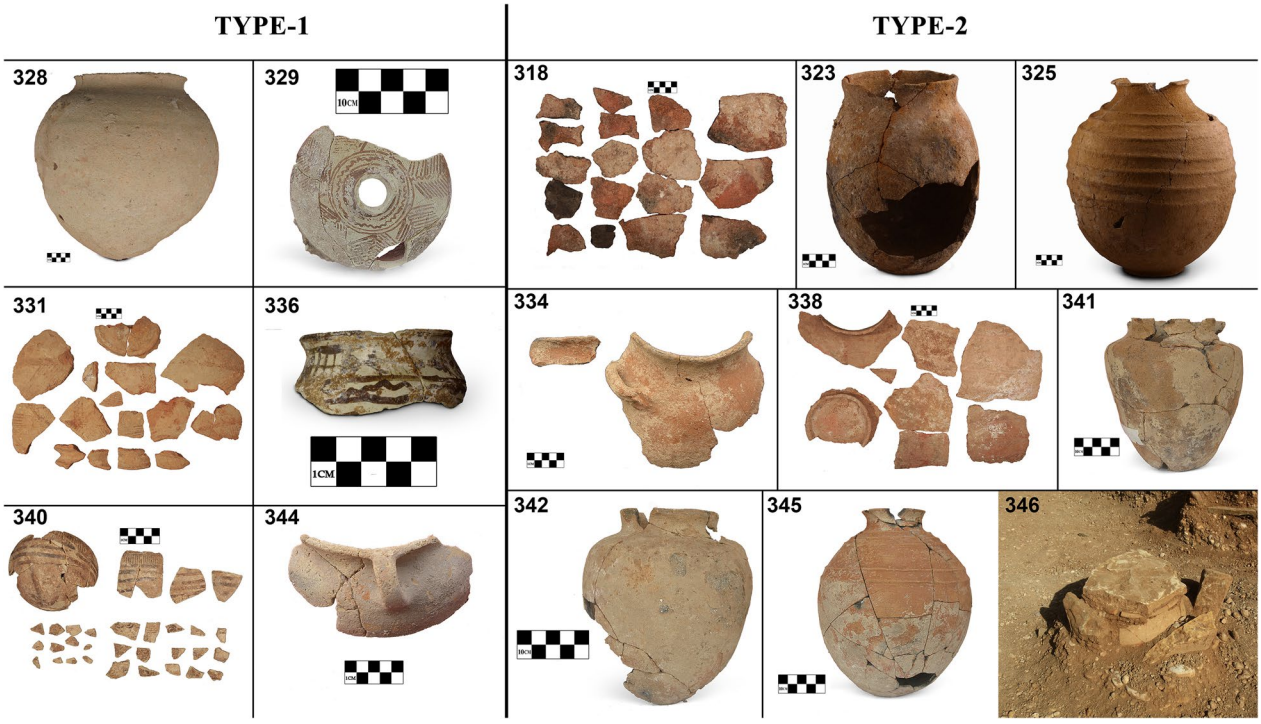


**Fig. 3** Images of some representative potteries analysed in this study and belonging to the two types described in the text

More potteries belonged to TYPE-2 as these constituted the majority of the ceramic objects found in the graveyard.

### Analytical methods

#### *Chemical, mineralogical and textural characterization*

All samples were broken in three parts: one was milled and powdered for chemical and mineralogical analyses, another was used to prepare thin sections for their observation under the microscope, and a third and larger part was used for the hydric tests.

The chemical composition (major elements) was determined by X-ray fluorescence (XRF) using a PANalytical Zetium compact spectrometer with a Rh anode and 4 kV X-ray generator and measurement accuracy of ±0.05%. 6 g per sample were milled to powder and then analysed.

The mineralogical composition was identified by means of powder X-ray diffraction (XRD) using a PANalytical X'Pert PRO diffractometer. The working conditions were: CuKα radiation (λ = 1.5405 Å), 45 kV voltage, 40 mA current, 3 to 60° 2θ explored area and 0.01 2θ/s goniometer speed. Samples were milled in an agate mortar to a particle size of < 0.063 mm and then analysed. The interpretation of diffractograms was made using XPowderX software [45].

To determine the petrographic characteristics of pottery sherds, thin sections from each sample were observed under polarized light microscopy (PLM) using a Zeiss Primotech microscope.

The micro-textural characterization was studied on carbon-coated polished thin sections using a field emission scanning electron microscope (FESEM) with a focused ion beam Carl Zeiss STM (AURIGA Series), coupled with EDS microanalysis.

#### *Hydric behaviour*

Hydric tests were carried out to assess the absorption and drying rate of the samples over time, which can be indirectly related to their durability, as the majority of decay processes involve a flow of water through pores and fissures [46]. Free ($A_b$) and forced (i.e. under vacuum) water absorption ($A_f$) and drying ($D_i$) tests were carried out according to UNE-EN 13,755 [47] and NORMAL 29/88 [48] standards respectively. These tests evaluated the degree of pore interconnectivity (Ax) [49], the open porosity ($P_o$), the apparent ($\rho_a$) and real densities ($\rho_r$) according to the RILEM standard [50]. Hydric tests were performed under controlled thermo-hygrometric conditions (20 ± 2 °C and 50 ± 5% relative humidity) and using deionized water. The only deviations from the EN, Normal and RILEM standard procedures concern the shape and size of samples, as single and irregular fragments of different size, shape and weight were tested. One sample per pottery was used to determine the hydric behaviour.

## Results and discussion

### Chemical composition

All samples are rich in $SiO_2$ that varies from 41.8% (sample 319) to 59.8% (sample 347). $Al_2O_3$ is rather high especially in samples 319, 338, 328 and 332 wherein it exceeds 25%. Iron varies from 4.5% (sample 332) to 9.1% (sample 323) (Table 1). Following Maniatis and Tite [51], ceramics have been divided into two groups on the basis of their CaO content: high calcareous ceramics (thereafter HCC) and low calcareous ceramics (thereafter LCC), where CaO content is respectively over or below 6% (Table 1). If we relate the classification based on the CaO content with that made on the basis of the macroscopic appearance of samples, LCC samples belong almost exclusively to TYPE-2 of potteries (see Fig. 3), with sample 328 as the only exception. HCC samples, instead, seem to belong equally to TYPE-1 and TYPE-2 of potteries.

Among HCC samples, CaO is particularly high in sample 163 where ~22% is reached. In addition, MgO content is usually higher in HCC ceramics compared to LCC. These samples also show a generally but not always higher LOI content than LCC ones (Table 1) since this value can be linked both to the release of $CO_2$ from carbonates and to the dehydroxylation of phyllosilicates [52]. The other oxides are very low, only reaching sometimes 2%, as it is the case of $K_2O$ (Table 1).

### Mineralogy

XRD results are given in Table 2 and the X-ray diffraction patterns of two of the most representative LCC and HCC potteries are shown in Fig. 4.

LCC potteries are rich in quartz. Na-plagioclase and muscovite were detected in almost all samples. Calcite was also detected in many samples, in some cases with small amounts. Less frequent are K-feldspar and hematite. Sample 328 is the only sample where muscovite was not detected and mullite was identified in its place, denoting a high firing temperature (not less than 1000 °C) for this ceramic that has caused a total replacement of this phyllosilicate by mullite [54]. On the contrary, sample 332 is characterized by the presence of both muscovite and chlorite, suggesting a very low firing temperature, below 750 °C according to Peters and Iberg [55]. Aragonite in sample 338 is of secondary origin and an organic process may have been involved in its formation [56, 57].

The mineralogy of HCC is quite different. Quartz was detected in all samples, though it is not always the main phase as in 163, 329 and 336 samples where diopside prevails (Table 2). This new silicate formed by the reaction

**Table 1** Elemental chemical composition of the pottery samples, expressed as major oxides (in wt%). LOI stands for loss on ignition

| | Sample code | Type | $SiO_2$ | $Al_2O_3$ | $Fe_2O_3$ | MnO | MgO | CaO | $Na_2O$ | $K_2O$ | $TiO_2$ | $P_2O_5$ | LOI |
|---|---|---|---|---|---|---|---|---|---|---|---|---|---|
| LCC | 318 | TYPE-2 | 59.07 | 16.05 | 8.11 | 0.14 | 2.70 | 2.99 | 0.87 | 2.29 | 0.99 | 0.29 | 6.50 |
| | 323 | TYPE-2 | 56.59 | 17.88 | 9.11 | 0.12 | 2.04 | 3.69 | 0.85 | 2.10 | 1.08 | 0.33 | 6.21 |
| | 324 | TYPE-2 | 54.44 | 18.22 | 8.83 | 0.08 | 3.66 | 3.69 | 0.87 | 2.46 | 0.91 | 0.23 | 6.62 |
| | 326 | TYPE-2 | 53.80 | 18.01 | 7.89 | 0.12 | 1.73 | 5.98 | 0.70 | 1.78 | 1.16 | 0.36 | 8.46 |
| | 328 | TYPE-1 | 54.50 | 29.95 | 5.50 | 0.01 | 0.96 | 2.83 | 0.11 | 1.61 | 1.34 | 0.16 | 3.04 |
| | 330 | TYPE-2 | 57.83 | 16.05 | 7.88 | 0.12 | 2.42 | 4.18 | 0.95 | 2.22 | 0.94 | 0.29 | 7.12 |
| | 332 | TYPE-2 | 51.65 | 35.55 | 4.48 | 0.01 | 0.87 | 1.28 | 0.07 | 0.78 | 1.87 | 0.12 | 3.31 |
| | 334 | TYPE-2 | 54.73 | 15.62 | 8.24 | 0.12 | 3.23 | 5.16 | 0.59 | 1.98 | 0.95 | 0.22 | 9.14 |
| | 338 | TYPE-2 | 51.97 | 27.19 | 5.25 | 0.01 | 0.89 | 4.51 | 0.19 | 0.78 | 1.37 | 0.13 | 7.71 |
| | 341 | TYPE-2 | 58.74 | 16.89 | 8.92 | 0.14 | 2.61 | 2.78 | 0.75 | 2.10 | 1.07 | 0.38 | 5.61 |
| | 346 | TYPE-2 | 57.65 | 14.17 | 8.60 | 0.17 | 3.78 | 5.95 | 0.92 | 2.14 | 0.93 | 0.56 | 5.14 |
| | 347 | TYPE-2 | 59.79 | 16.72 | 8.25 | 0.13 | 3.31 | 3.51 | 0.75 | 2.12 | 1.10 | 0.28 | 4.05 |
| HCC | 163 | TYPE-1 | 43.91 | 11.34 | 5.82 | 0.08 | 5.02 | 21.70 | 0.85 | 0.70 | 0.68 | 0.20 | 9.69 |
| | 319 | TYPE-2 | 41.80 | 25.14 | 6.67 | 0.01 | 1.15 | 7.61 | 0.08 | 0.38 | 1.24 | 0.17 | 15.76 |
| | 322 | TYPE-1 | 48.36 | 15.95 | 8.17 | 0.06 | 5.52 | 10.48 | 0.54 | 0.87 | 0.88 | 0.33 | 8.84 |
| | 325 | TYPE-2 | 49.78 | 15.62 | 7.40 | 0.07 | 5.05 | 12.63 | 0.15 | 1.13 | 0.77 | 0.26 | 7.13 |
| | 329 | TYPE-1 | 47.23 | 14.96 | 8.14 | 0.10 | 6.77 | 13.95 | 0.17 | 0.54 | 0.88 | 0.29 | 6.96 |
| | 331 | TYPE-1 | 53.95 | 14.98 | 7.28 | 0.13 | 3.17 | 8.28 | 0.48 | 1.88 | 0.92 | 0.46 | 8.47 |
| | 336 | TYPE-1 | 45.32 | 15.29 | 8.10 | 0.10 | 4.82 | 16.58 | 0.36 | 1.01 | 0.89 | 0.22 | 7.30 |
| | 337 | TYPE-2 | 48.44 | 16.00 | 8.03 | 0.11 | 3.79 | 12.69 | 0.19 | 1.33 | 0.99 | 0.20 | 8.22 |
| | 340 | TYPE-1 | 52.96 | 16.92 | 8.78 | 0.15 | 3.93 | 8.27 | 0.18 | 0.94 | 1.09 | 0.32 | 6.46 |
| | 342 | TYPE-2 | 52.30 | 14.29 | 6.96 | 0.12 | 3.24 | 8.78 | 0.75 | 1.88 | 0.92 | 0.22 | 10.53 |
| | 344 | TYPE-1 | 49.46 | 13.44 | 6.65 | 0.07 | 3.31 | 14.32 | 0.37 | 1.52 | 0.79 | 0.33 | 9.74 |
| | 345 | TYPE-2 | 55.16 | 15.96 | 7.32 | 0.06 | 2.80 | 6.08 | 0.60 | 2.02 | 0.93 | 0.22 | 8.85 |

of quartz with dolomite, suggesting a firing temperature of 950 °C or higher [52]. Calcite, also detected in these samples, must be of secondary origin due to prolonged burial of the ceramics. The total decomposition of calcite is completed at around 850 °C [58], therefore this phase cannot coexist together with diopside and anorthite, which crystallize over 1000 °C [52, 59]. However, it is worth pointing out that variables such as the time taken to fire the potteries, the size of calcite grains in the raw material and the $CO_2$ partial pressure in the oven during firing can shift calcite decomposition process towards higher temperatures [60, 61]. Calcite might be of primary origin in samples 342, 345, 331 and 319. The latter, where calcite is the main phase together with chlorite, could have been fired at a temperature not higher than 800 °C [62].

## Petrography

The existence of two types of ceramics on the basis of the macroscopic observation is maintained after the observations of the microstructure of samples under the optical microscope.

On the one hand, TYPE-1 potteries are characterised by a very fine-grained clayey matrix in which fine particles of quartz and feldspars are scattered. Small and large calcite grains and limestone particles with sharp edges are also visible in these samples, indicating that they were added to the ceramic paste deliberately, probably by crushing local limestone and using the resulting coarse-grained powder as temper (Fig. 5). Small particles of quartz and red-brown particles (probably iron compounds) are also visible in the matrix of some of the samples belonging to TYPE-1. On the other hand, TYPE-2 potteries are characterised by the existence of a black core (Fig. 6). The matrix of these samples is characterised by large pores that could have been generated after burning of straw or other plants added as temper in the pottery paste [62]. Large calcite grains (up to 0.5 mm in size in some samples) with cleavage and angular edges were also observed, suggesting that powdered limestone fragments were used as temper [63–65].

In some samples of the two types of potteries, the calcite grains do not show their typical birefringence but they appear brown in colour (see samples 163, 326, 337 and 347 in Figs. 5 and 6), indicating carbonate breakdown due to firing process [52]. Clayey inclusions (lumps) and small calcite grains with round shape are more visible in potteries with bright (yellowish hue) core (TYPE-1)

**Table 2** Mineralogical composition of the archaeological potteries

| | Sample code | Type | Qz | Ms | Chl | Pl | Fs | Cal | Ar | Hem | Mul | Di |
|---|---|---|---|---|---|---|---|---|---|---|---|---|
| LCC | 318 | TYPE-2 | xxx | xx | | xx | | x | | | | |
| | 323 | TYPE-2 | xxx | x | | xx | x | x | | | | |
| | 324 | TYPE-2 | xxx | xx | | xx | x | xx | | x | | |
| | 326 | TYPE-2 | xxx | xx | | x | | x | | | | |
| | 328 | TYPE-1 | xxx | | | | | xx | | x | xx | |
| | 330 | TYPE-2 | xxx | x | | xx | x | x | | x | | |
| | 332 | TYPE-2 | xxx | xx | | | | | | | | |
| | 334 | TYPE-2 | xxx | x | xx | xx | | x | | | | |
| | 338 | TYPE-2 | xx | x | | | | x | x | | | |
| | 341 | TYPE-2 | xxx | x | | x | x | | | tr | | |
| | 346 | TYPE-2 | xxx | x | | xx | | x | | x | | |
| | 347 | TYPE-2 | xxx | tr | | x | x | tr | | | | |
| HCC | 163 | TYPE-1 | x | | | xx | | xx | | | | xxx |
| | 319 | TYPE-2 | xx | | xx | | xx | xxx | | | | |
| | 322 | TYPE-1 | xxx | tr | | | | x | | x | | xxx |
| | 325 | TYPE-2 | xx | | | xx | | x | | x | | xx |
| | 329 | TYPE-1 | xx | | | | | | | x | | xxx |
| | 331 | TYPE-1 | xxx | x | | | xx | xx | | x | | |
| | 336 | TYPE-1 | xx | | | xx | | x | | | | xxx |
| | 337 | TYPE-2 | xx | | | xx | | x | | x | | xx |
| | 340 | TYPE-1 | xx | | | xx | | | | x | | xx |
| | 342 | TYPE-2 | xx | x | x | xx | | xx | | tr | | |
| | 344 | TYPE-1 | xx | | | xx | | xx | | x | | xx |
| | 345 | TYPE-2 | xxx | x | | xx | | x | | | | |

*Qz* quartz, *Ms* muscovite; *Chl* chlorite, *Pl* plagioclase, *Fs* K-Feldspar, *Cal* calcite, *Ar* aragonite, *Hem* hematite, *Mul* mullite, *Di* diopside. xxx = very abundant; xx = abundant; x = scarce; tr = traces. Mineral abbreviation after Whitney and Evans [53]

(Fig. 5). The presence of clay lumps in some samples may indicate an imperfect kneading of the raw materials [64, 66, 67].

### Microtexture

After the mineralogical study, some potteries were selected to be studied more in detail under FESEM. A general observation of samples with the same magnification enabled distinguishing coarser from finer textures. In general, the latter are present in HCC potteries, which are characterized by grains no bigger than 10 µm (Fig. 7a), whilst the former appear in LCC potteries, which have grains larger than 50 µm (Fig. 7b).

In some samples, the orientation of phyllosilicates and the presence of elongated pores were observed, suggesting a pressure exerted on the ceramic bodies during moulding (Fig. 7a). Clay lumps, already identified by PLM, are present in almost all samples.

Quartz grains with angular morphology and phyllosilicates with marked exfoliation along basal plane were observed. Phyllosilicate sheets sometimes tend to be separated due to dehydroxylation, being on occasions accompanied by the enrichment in Fe of several laminae (Fig. 7c). Calcite is observed in many samples with angular morphology, confirming the observations carried out under optical microscopy. Nanometric pores inside the calcite crystals of some LCC samples were observed, suggesting an early stage of decomposition and the release of $CO_2$ (Fig. 7d), as demonstrated by Rodriguez Navarro et al. [58]. Figure 7d highlights that these nanometric pores are rhombic-shaped, maintaining the rhombohedral cleavage of the crystal. Nanoporosity can be observed on all the surface of calcite crystals, although it is mainly concentrated along the cleavage surfaces as they are weaker areas of the crystals. In some samples, a thin layer of sparitic calcite has been observed covering the surfaces or inside the pores, as a result of the burial of ceramics, as suggested by XRD results. In some samples of the HCC ceramics, thin bright reaction rims around carbonates were observed, denoting the formation of some new silicate phases.

Sample 329 from the HCC group differs from the others since its matrix is characterised by ellipsoidal pores with Ca-rich borders (Fig. 7e), which are very likely to

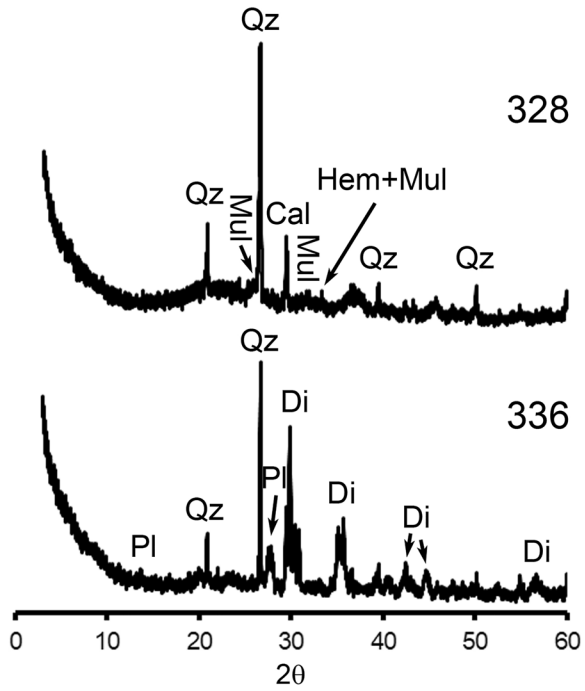


**Fig. 4** X-ray diffraction patterns of 328 and 336 potteries as the most representative samples from LCC and HCC groups, respectively. *Qz* quartz, *Cal* calcite, *Mul* mullite, *Hem* hematite, *Pl* plagioclase, *Di* diopside. Mineral abbreviation after Whitney and Evans [53]

correspond to shells (of bivalves, probably). This might be indicative of the use of a different raw material for the manufacturing of this pottery, most likely a bivalves-rich limestone from Asmari Formation. Nanometric to micrometric reaction rims have been observed in these ellipsoidal borders, with the formation of gehlenite ($Ca_2Al(AlSi)O_7$) and diopside ($CaMgSi_2O_6$) (Fig. 7f and inset with EDS spectra). Quartz seems to be involved in this reaction, as its grain edges show smooth surfaces.

Hematite ($Fe_2O_3$) grains are scattered in the matrix, showing in some cases a framboidal morphology (Fig. 7 g) that has to be related with the original presence of pyrite crystals. It is known that during the firing of ceramics framboidal pyrite loses sulphur, due to the thermal decomposition of sulphide at 588 °C, and finally turns into hematite under oxidising conditions [68].

As a general feature found in the matrix of samples, the shape of the pores is irregular. In the case of samples with a coarser matrix, the large grains are surrounded by an interparticle porosity. Samples that suffered a partial vitrification show the development of a secondary porosity in the matrix characterised by micrometric pores with a rounded or elongated morphology and smoothed surfaces (Fig. 7h). In the same samples where a secondary porosity was observed, the presence of new silicate phases, such as diopside in samples 322 and 329 and K-feldspar ($KAlSi_3O_8$) in sample 347, was also detected by XRD, confirming that these samples were fired at high temperature.

Small crystals of pyrite ($FeS_2$), rutile ($TiO_2$), apatite ($Ca_5(PO_4)_3(OH,F,Cl)$), ilmenite ($Fe^{++}TiO_3$), zircon ($ZrSiO_4$), titanite ($CaTiSiO_5$) and chromite ($Fe^{++}Cr_2O_4$) were also observed and identified by EDX, as accessory phases scattered in the matrix of some samples. These phases could not be detected by XRD due to their small concentrations.

### Hydric behaviour

Only samples 334 and 342 could not be studied due to their very small weight. The studied ceramics show great variability with respect to their ability to absorb water, obtaining values of free water absorption ($A_b$) ranging from 13% (sample 338) to 62% (sample 340). HCC samples generally absorb more water reaching an average $A_b$ value almost twice than that of LCC samples. The same trend is maintained after forced water absorption ($A_f$).

In both groups of ceramics there are samples with well-connected pores (i.e., with low Ax values), the best one being sample 341 (LCC group), and others with a tortuous pore network, as it is the case of sample 319 (HCC group), with the highest Ax value among all samples. Although there is not a clear tendency, it seems that HCC samples have a worse-connected pore system. To this respect, as discussed above, the decomposition of carbonates in HCC potteries yielded the development of nanoporosity that might be responsible for the worse interconnection compared to LCC samples.

Another parameter to be considered is the drying index (Di) since porous materials that dry quickly, and therefore retain less water, are generally more durable [69]. Di values are similar between the two groups indicating the same drying behaviour.

Regarding porosity ($P_o$), HCC are the most porous ceramics, with sample 340 that reaches about 60%. On the contrary, samples 338 and 318, both belonging to LCC ceramics, are the least porous with a value of $P_o$ of 25.6%. As the porosity of the ceramic increases, the greater becomes difference between $\rho_a$ and $\rho_r$. Thus, the high porosity of sample 340 is reflected in the very low value of $\rho_a$ measured. The higher $\rho_a$ values found in some samples (i.e., mainly those belonging to LCC group) might imply the achievement of a greater vitrification of their matrix [70].

## Pottery technology and provenance

Results of the multi-analytical study carried out on the pottery sherds from Deh Dumen have shown very interesting aspects of the pottery technology. Analyses

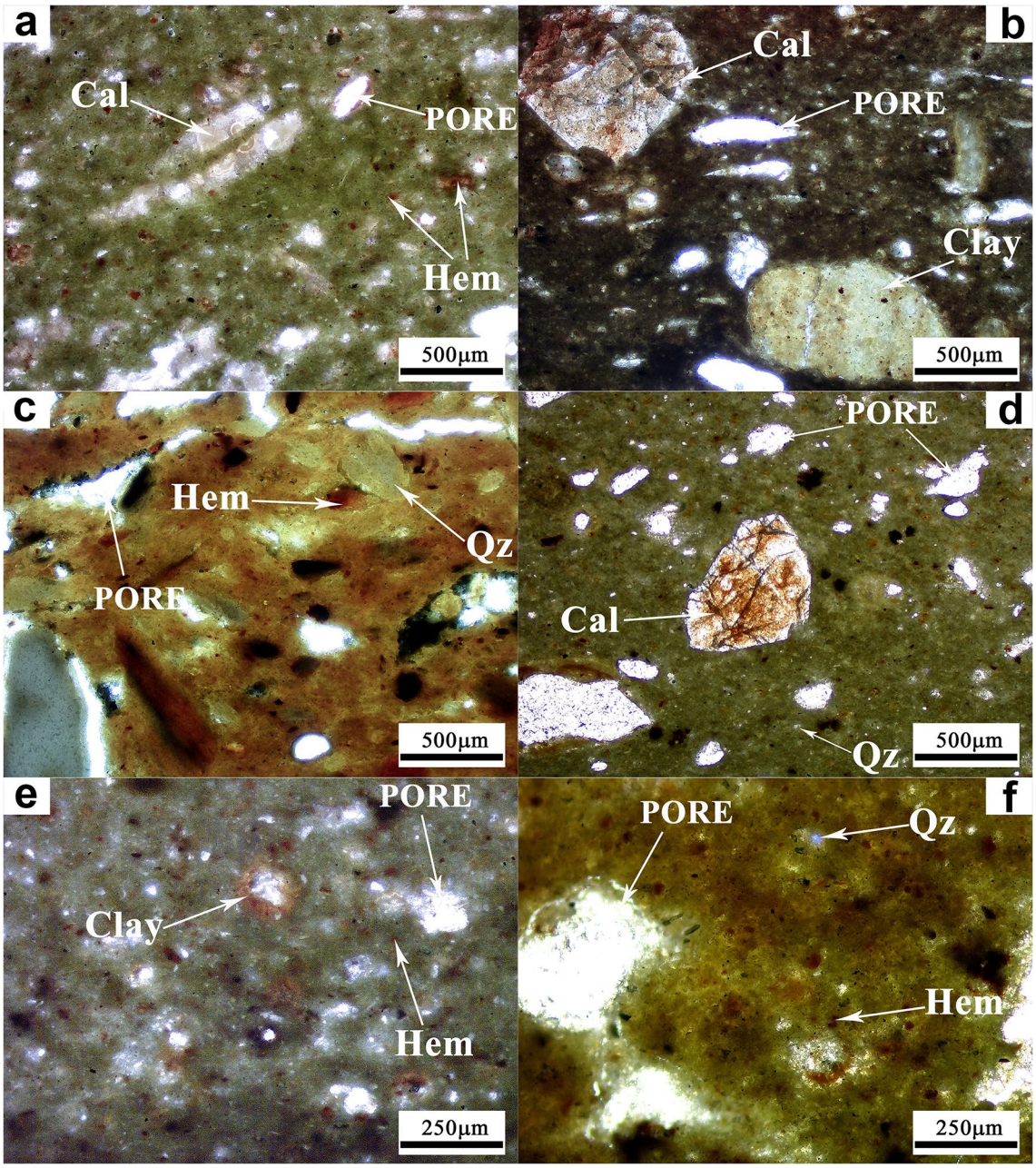


**Fig. 5** Optical microscopy images of some selected samples from the TYPE-1 potteries from Deh Dumen (bright yellowish hue fabric) in which clay matrix, high porosity and small particles/grains of quartz, hematite and large particles/grains of calcite, stone fragments (quartz) and clayey inclusions are visible (*Cal* calcite, *Qz* quartz, *Hem* hematite, *Clay* clayey inclusion). Minerals abbreviations after Whitney and Evans [53], **a** sample 163; **b** sample 322; **c** sample 328; **d** sample 329; **e** sample 336; **f** sample 340

revealed that there is no remarkable difference between the two types of potteries (TYPE-1 and TYPE-2), from the chemical, mineralogical and physical points of view, although they were classified as HCC and LCC according to their CaO concentration. The amount of CaO and MgO is higher in majority of TYPE-1 potteries, while $Fe_2O_3$ and $K_2O$ are higher in most of the samples from TYPE-2. The mineralogical composition shows in most of samples a wide range of phases such as quartz, muscovite, plagioclase and calcite, as well as other minor phases. One interesting aspect is the identification of diopside in HCC samples denoting a high firing

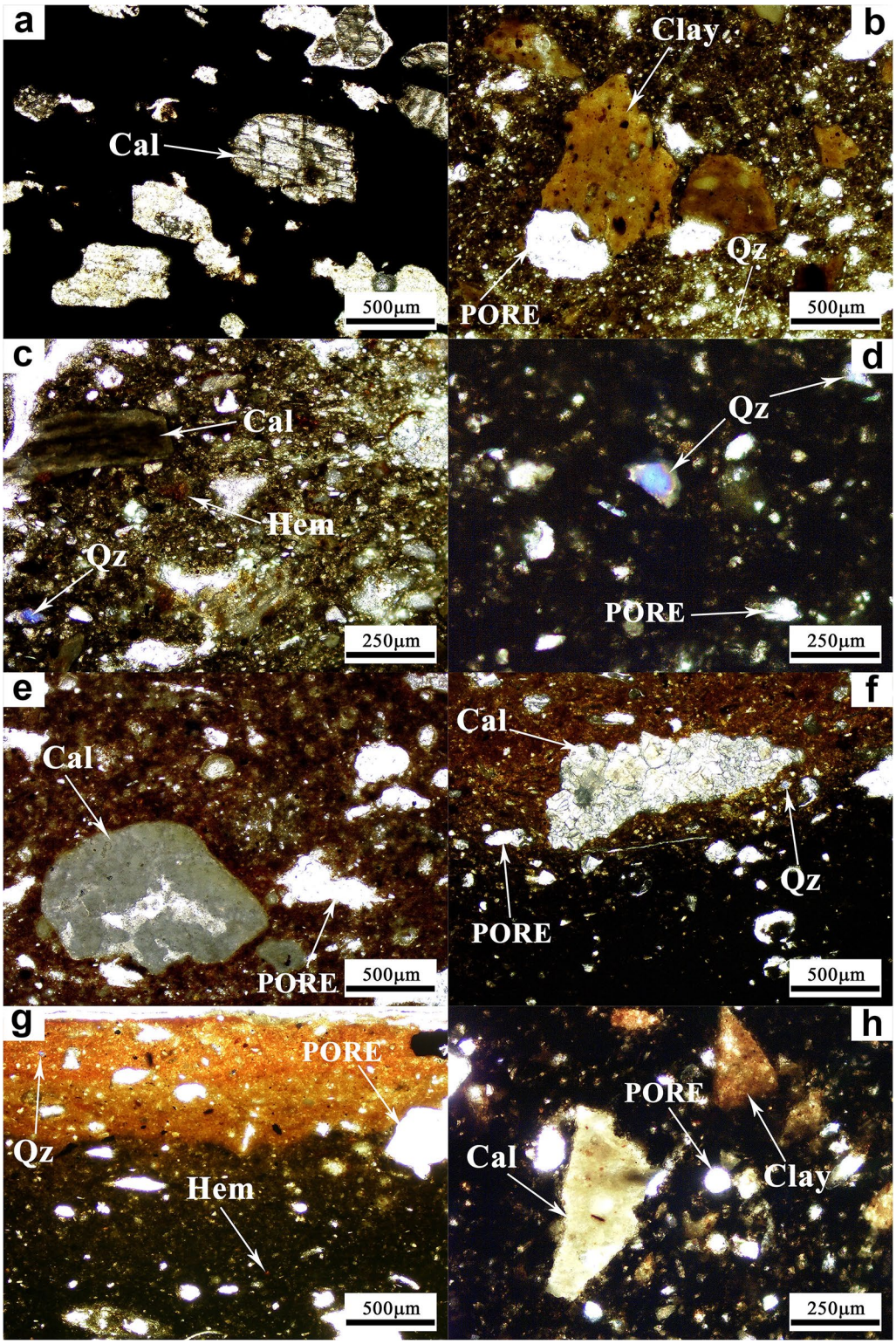


**Fig. 6** Optical microscopy images of some selected samples from TYPE-2 potteries from Deh Dumen **(**sandwich-like fabric) within which two different orange-red surface and black core are visible. High porosity and small particles/grains of quartz, hematite and large particles/grains of calcite, stone fragments (quartz) and clayey inclusions are visible (*Cal* calcite, *Qz* quartz, *Hem* hematite, *Clay* clayey inclusion). Minerals abbreviations after Whitney and Evans [53]. **a** sample 319; **b** sample 323; **c** sample 326; **d** sample 330; **e** sample 337; **f** sample 334; **g** sample 345; **h** sample 347

temperature. The same potteries also show a higher ability of absorbing water.

The manufacturing technology of Deh Dumen potteries was a traditional procedure widely used by the prehistoric potters in the Iranian Plateau. Common raw materials such as clay and temper from Asmari Formation were used for the manufacture of ceramics, moulding the clayey paste with the usual shapes of potteries found in western and south-western Iran from the third millennium BC, and finally firing them at a temperature not high enough to achieve high-temperature phase reactions. The results obtained in this research indicate that the few macroscopic differences observed in the potteries, which have led to their classification in two different types including bright yellowish hue fabric and sandwich-like fabric, might be due to either the use of different raw material sources or the existence of different production centres.

Organic and inorganic tempers were added to the raw material for the ceramic production. Organic temper was probably straw, which was added to reduce the shrinkage of the clayey material during drying, as observed in prehistoric potteries of the Iranian Plateau from the Neolithic period to the Iron Age [16, 59, 71, 72]. The use of straw gave rise to higher porosity in many of the Deh Dumen potteries, under the form of large holes generated at the earliest steps of firing, as microscopic observations and physical tests revealed. Therefore, the majority of the Deh Dumen potteries can be considered as "straw-tempered coarse pottery", together with limestone and clay lumps fragments, the latter ones used as inorganic tempers. Only few pottery vessels, mainly belonging to TYPE-1, are instead characterized by a fine texture with small pores.

The presence of low-temperature phases such as calcite in the majority of potteries indicates firing temperature lower or around 800 °C. Evidences of slightly higher firing temperatures have been observed in the microstructure of some samples where lower birefringence and darkening of carbonate grains were detected. It is worth highlighting that the size of carbonate grains has a great influence on their thermal decomposition, as large calcite fragments, as those observed in some of the studied potteries, need temperatures over 800 °C to be totally decomposed [63].

TYPE-2 potteries show a matrix with an orange-red colour near the surface and a darker colour inside, the core being almost black in some cases, similarly to other ancient potteries from different regions. According to literature, the black core in a ceramic is defined as sandwich-like structure and is attributed to the following phenomena [61, 73–76]:

- High proportion of $Fe^{2+}/Fe^{3+}$, especially in the presence of magnetite ($Fe_3O_4$) and wüstite (FeO) in the pottery paste (unfired clay).
- Presence of unburnt carbon particles in the structure of pottery.
- Firing of the pottery under reducing conditions with a cooling stage in oxidising conditions leading to presence of the trivalent iron ion in the red surface and the reduced iron oxides such as FeO or $Fe_3O_4$ in the black core.
- Firing of raw material rich in organic matter under oxidising conditions.
- Short firing duration and low temperatures hampering a complete oxidation within the ceramic body.

Nevertheless, the analytical studies suggest that the most probable reason for the formation of sandwich-like fabric is linked to the reducing conditions during firing, which could have originated from the formation of carbon and FeO, while the red colour of the surface is assigned to the crystallization of hematite [76, 77].

Based on the composition and microstructure of the potteries from Deh Dumen, we may conclude that the formation of black core can be attributed to both the addition of organic matter (such as straw) to the clayey material and an incomplete oxidizing atmosphere (or reducing condition) in the kiln.

It is worth highlighting that there are few analytical studies of ceramic production in southern and

(See figure on next page.)

**Fig. 7** BSE images performed on selected samples: **a** general appearance of a ceramic with small grain size (sample 319). Note the same orientation of phyllosilicates and fissures; **b** general appearance of a ceramic characterized by coarse quartz grains with angular morphology (sample 328); **c** detailed image in which a phyllosilicate enriched in iron can be seen (sample 323). The phyllosilicate shows separation along basal planes due to dehydroxylation. The white arrow indicates the presence of a small rutile crystal; **d** detailed image of a calcite crystal with polygonal pores mainly located along the cleavage planes (sample 334); **e** presence of an ellipsoidal pore that suggests the previous existence of carbonatic shell (sample 329). The brighter border indicates a reaction between carbonate and the matrix; **f** detailed image of a reaction rim observed in Fig. 7e: quartz grains with smoothed edges and newly-formed calcium silicates (see inset with EDS spectra); **g** clays sheets mould around harder quartz grain. A brighter Fe-rich framboid can be seen (sample 332); **h** development of secondary porosity in the matrix (sample 347), with micrometric rounded to elongated pores

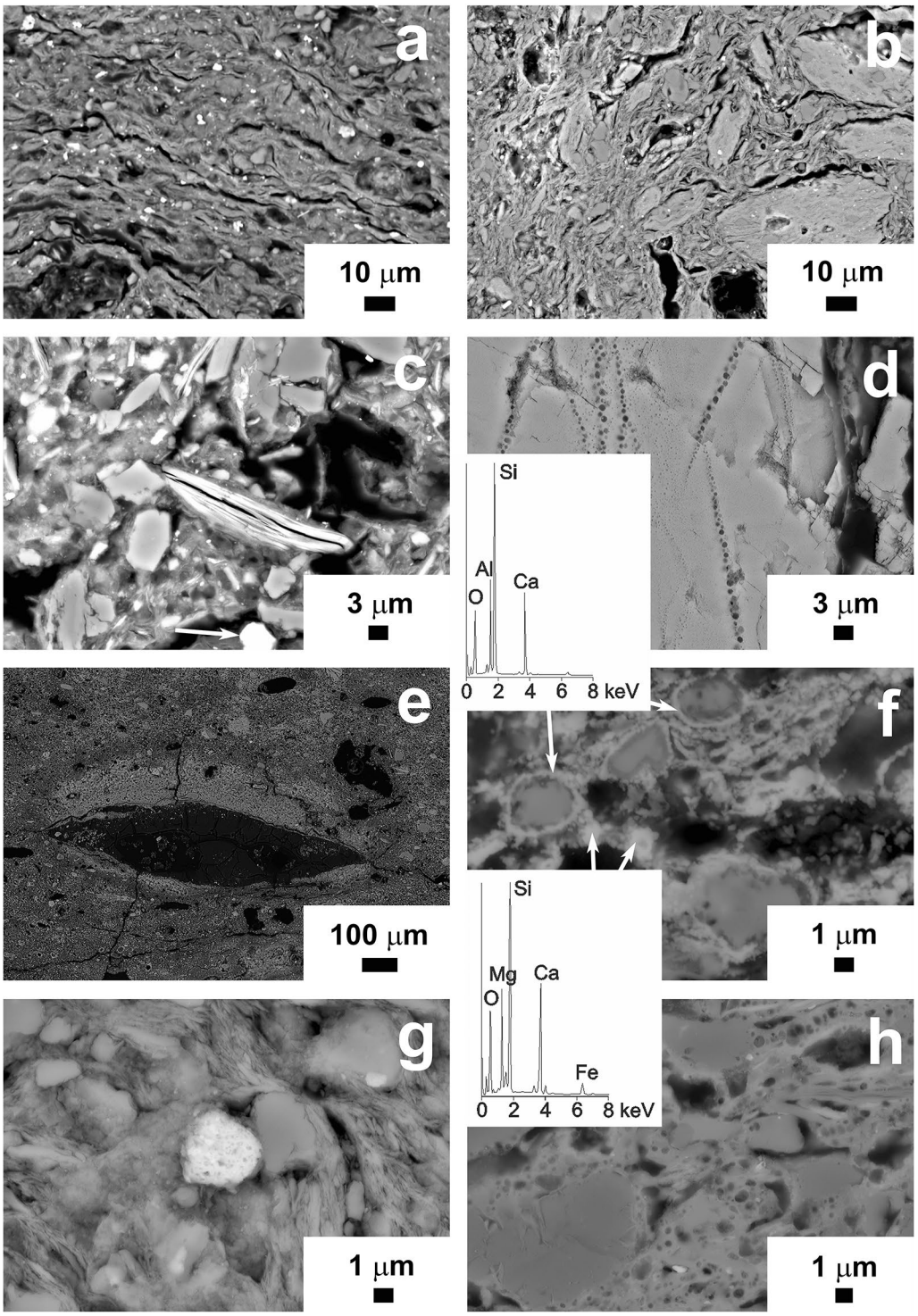


**Fig. 7** (See legend on previous page.)

south-western Iran compared to other Iranian regions. This is the case of the prehistoric site of Rahmatabad (fifth millennium BC) [16], the potteries from the late Neolithic period of Susa (last fifth/early fourth millennium BC) [78], and the potteries from the middle Elamite sites (second millennium BC) of Haft Tappeh

and Chogha Zanbil [29, 30]. These ceramics show differences from a chemical point of view with those from Deh Dumen, especially in some major constituents such as $Al_2O_3$, CaO and $Fe_2O_3$, which are in a wider range of concentration in the potteries of Deh Dumen. Figure 8 compares the main chemical elements measured in the potteries from Deh Dumen graveyard with those of potteries from the aforesaid prehistoric sites in southern and south-western Iran. Figure 8a shows higher samples dispersion of Deh Dumen potteries with respect to those from the other sites when $Al_2O_3$ and $K_2O$ are compared. The dispersion of Deh Dumen pottery is maintained in Fig. 8b and c where scatter plots of CaO versus MgO and $Fe_2O_3$ versus $Na_2O + K_2O$ are shown in wt%. Even though no remarkable differences were obtained, the chemical composition of the studied ceramics enables distinguishing and discriminating them from those of other archaeological areas.

Based on the scatter plots, many of TYPE-2 pottery sherds show similar composition while some deviations are visible in some samples. On the other hand, TYPE-1 pottery shreds are more variable and some of them have correlation with samples of the other type. The scatter plot of $Al_2O_3$ versus $K_2O$ (Fig. 8a) shows that the majority of both types of pottery sherds present significant correlation while four samples are out from their compositional range (one sample from TYPE-1 and three samples from TYPE-2). Moreover, TYPE-2 samples show strong correlation with those from Rahmatabad and Susa. Figure 8b (CaO versus MgO) reveals that most of Deh Dumen samples of TYPE-2 differ greatly from the potteries of other sites whereas some samples of the other type are similar with samples from different sites and show a wide range of chemical composition. This scatter plot shows a partially linear proportion between CaO and MgO in all samples, although this proves that the carbonatic stones from Deh Dumen may were different from the other sites from chemical point of view or the Ca-Mg content of the used clay was lower than the other clay resources. Finally, the $Fe_2O_3$ versus $Na_2O + K_2O$ scatter plot (Fig. 8c) presents two groups including samples with higher alkali metals (from TYPE-2) and samples with lower alkali metals (from both types). The $Fe_2O_3$ content does not show a trend in both types of pottery sherds from Deh Dumen. Although this comparative analysis cannot prove a strong relationship between the potteries from Deh Dumen and other sites, it still demonstrates the variability of chemical composition in the Deh Dumen potteries compared to the others. This difference might be due to a different pottery technology (probably a local technology) in the Deh Dumen graveyard, by using local resources or different clay resources, which apparently differ from those from other archaeological sites. The partial correlation between some pottery sherds from Deh Dumen with those from other sites such as Rahmatabad and Susa may suggest the use of similar resources to produce these objects. However, the available data cannot support a connection or same production centre for Deh Dumen and other sites.

The comparison between the graves of Deh Dumen with archaeological sites of western and south-western Iran during third millennium BC, especially those of Pusht-i Kuh (Luristan) as well as Susa and Susiana plain settlements [32, 79–82], indicate a close relationship between the south of Zagros fold and thrust belt (Deh Dumen area) and central Zagros (Luristan) and Iranian lowlands (Susiana plain). It seems that that most of the pottery sherds from the Deh Dumen graveyard were produced by means of a local and traditional pottery manufacturing technique, whilst others may have been produced in different places and workshops and transported into the site. Consequently, it can be hypothesized that Deh Dumen potteries were either imported from other regions by nomads and placed within graves as ritual offers, or produced by nomads of the region itself using local resources, though with artistic styles similar to those of Susa and Luristan. The second hypothesis is more likely because the powdered limestone was available and easily accessible in the Zagros fold and thrust belt region [83–85], especially near the Khersan river where the Deh Dumen graveyard is located.

## Conclusions

A multi-analytical approach on a series of potteries from the Bronze Age graveyard of Deh Dumen (south-western Iran) dated to half of the third millennium BC, were undertaken to identify the technology production. The potteries from the site were divided into those with bright yellowish hue fabric (TYPE-1) and those with sandwich-like fabric (TYPE-2). Chemical and mineralogical analyses revealed that they were manufactured by an ordinary (and partially traditional) method, consisting in using clayey materials with significant amount of quartz, small fragments of limestone and straw as temper, firing the pottery in a kiln under an incomplete oxidising atmosphere, leading to TYPE-2 structure.

The TYPE-1 of potteries is characterized by a fine clayey matrix with small quartz grains and other silicate phases scattered in the matrix. These potteries have small calcite fragments and clayey inclusions and no evidence of sandwich-like structure is visible. Based on hydric tests and microscopic observations, potteries from TYPE-1 show high porosity due to the burning of straw tempers during firing. The TYPE-2 of ceramics does show a coarser matrix in which large calcitic grains and clayey lumps are visible. The porosity is

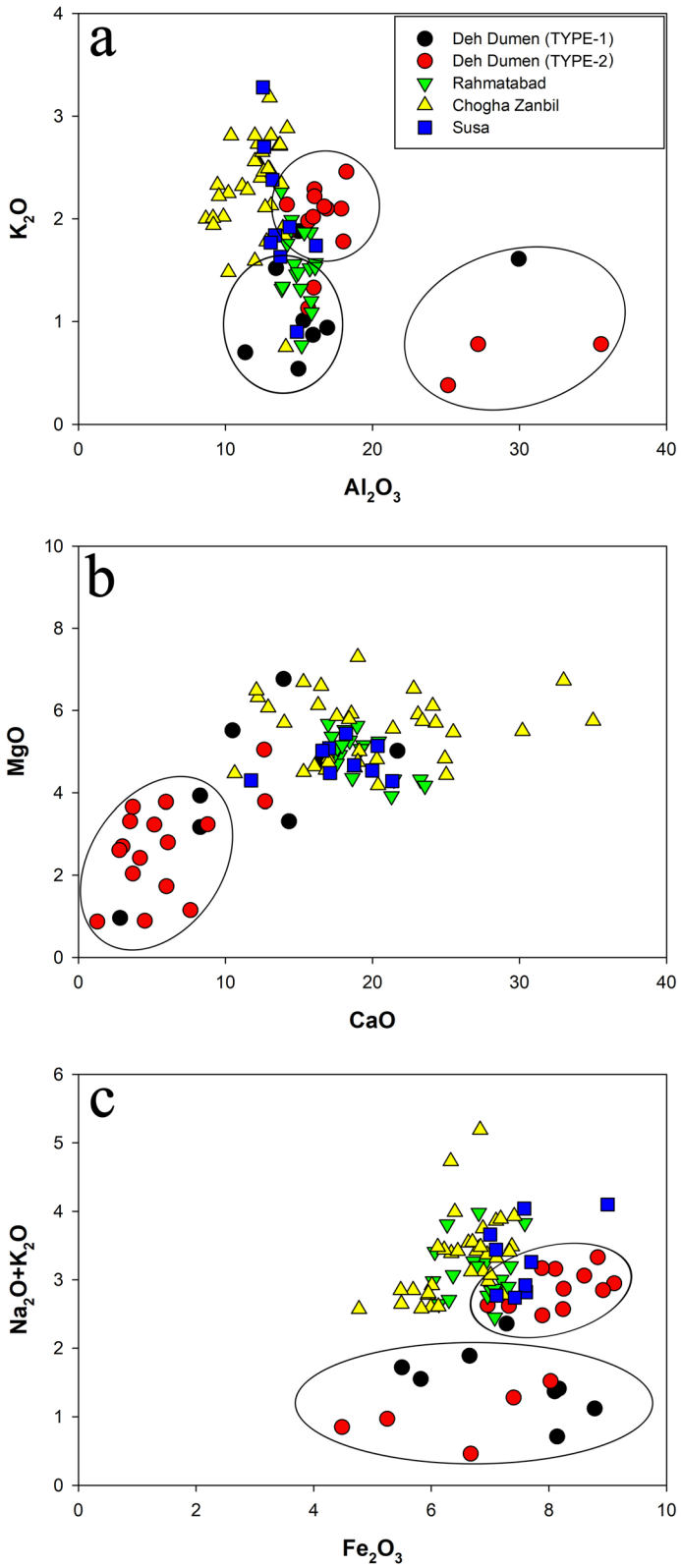


**Fig. 8** Scatter plots of some of the main chemical components of Deh Dumen potteries and of other archaeological sites from southern/south-western Iran; **a** $Al_2O_3$ vs. $K_2O$; **b** CaO vs. MgO; **c** $Fe_2O_3$ vs. $Na_2O + K_2O$, in wt%. Comparative data collected from references No. [16, 29, 78]

generally lower as well as the ability of the samples to absorb water. It should be pointed out that although the hydric tests highlighted some differences between the potteries from Deh Dumen, it is difficult to extrapolate these results to other ceramics from other archaeological areas.

The results of the analytical and comparative studies showed that it is possible that two types of potteries were produced in two places or workshops due to differences in their appearance as well as in their physical-chemical characteristics. It has been possible to classify the Deh Dumen potteries as local and imported materials, as significant number of them may have been produced in a region near the site with local raw materials and some other had been imported from south-western Iran such as the Susiana plain, according to archaeological evidences, to be used as ritual objects to place in the graves. It is worth noting that no evidence of pottery production (workshop/kiln) has been discovered in the region but based on the limestone fragments identified in the microstructure of the sandwich-like potteries, it is presumable that this type has been produced locally in a place within the Zagros mountain. The results of this preliminary research have shown the presence of different types of pottery (at least two types) in the site of Deh Dumen from third millennium BC but it is necessary to perform further analytical studies to the potteries to confirm this achievement.

**Abbreviations**

FESEM-EDS: Field emission scanning electron microscopy coupled with energy dispersive X-ray spectroscopy; XRD: X-ray diffraction; XRF: X-ray fluorescence; LOI: Loss on Ignition.

**Acknowledgements**

The Authors are grateful to Dr. Atefeh Shekofteh (Art University of Isfahan) and Mohammad Reza Rokni (RICHT-ICAR) for their valuable helps to perform this research. This study was funded by Junta de Andalucía Research Group RNM179 and by Research Project MAT2016-75889-R, as well as the Center for International Scientific Studies and Collaborations (CISSC), Ministry of Science, Research and Technology (MSRT), Iran. We thank the Centro de Instrumentación Científica of the University of Granada for the XRF and FESEM analyses.

**Authors' contributions**

OO contributed in the sampling and analytical works (petrography) and interpretation of the analytical data as well as preparing the draft of the manuscript; RN prepared the archaeological data of the site and samples and also contributed to sampling; GC contributed in the analytical works (FESEM) and interpretation of the analytical data as well as preparing and editing the manuscript; IE worked in the preparing samples for analyses and performing the chemical and physical analyses (XRD, XRF and hydric tests); AA contributed in preparing and editing the manuscript. All authors read and approved the final manuscript.

**Funding**

This research was funded by the Junta de Andalucía Research Group RNM179, the Spanish Research Project MAT2016-75889-R and the Iranian Center for International Scientific Studies and Collaborations (CISSC).

**Availability of data and materials**

The datasets used and/or analysed during the current study are available from the corresponding author on reasonable request.

## Declarations

**Competing interests**

The authors declare that they have no competing interests.

**Author details**

[1]Department of Conservation of Cultural and Historical Properties, Art University of Isfahan, Isfahan, Iran. [2]Researcher at Center for International Scientific Studies and Collaborations (CISSC), Ministry of Science, Research and Technology (MSRT), Tehran, Iran. [3]Department of Archaeology, University of Zabol, Zabol, Iran. [4]Department of Mineralogy and Petrology, University of Granada, Granada, Spain. [5]Department of Geography and Regional Science, University of Graz, Graz, Austria.

Received: 9 March 2021 Accepted: 29 June 2021
Published online: 08 July 2021

**References**

1. Majidzadeh Y. The Development of the Pottery Kiln in Iran from prehistoric to Historical Periods. Paléorient. 1975;3:207–21.
2. Azarnoush M, Helwing B. Recent archaeological research in Iran – Prehistory to Iron Age. AMIT. 2005;37:189–246.
3. Gregg MW, Thornton CP. A Preliminary Analysis of Prehistoric Pottery from Carleton Coon's Excavations of Hotu and Belt Caves in Northern Iran: Implications for Future Research into the Emergence of Village Life in Western Central Asia. International Journal of Humanities. 2012;19:56–94.
4. Nishiaki Y. A Radiocarbon Chronology for the Neolithic Settlement of Tall-i Mushki, Marv Dasht Plain, Fars, Iran. Iran. 2010;48:1–10.
5. Roustaei K, Mashkour M, Tengberg M. Tappeh Sang-e Chakhmaq and the beginning of the Neolithic in north-east Iran. Antiquity. 2015;89:573–95.
6. Dyson RH. CERAMICS I. The Neolithic Period through the Bronze Age in Northeastern and North-central Persia. In: Yarshater E, editor. Encyclopaedia Iranica, V, Fasc. 3, 1991. p. 266–275.
7. Voigt MM. CERAMICS II. The Neolithic Period in Northwestern Persia. In: Yarshater E, editor. Encyclopaedia Iranica, V, Fasc. 3, 1991. p. 275–276.
8. Mortensen P. CERAMICS III. The Neolithic Period in Central and Western Persia. In: Yarshater E, editor. Encyclopaedia Iranica, V, Fasc. 3, 1991. p. 276–278.
9. - Carter E. ČOḠĀ ZANBĪL, In: Yarshater E, editor. Encyclopaedia Iranica, VI/1, 1992. p. 9–13.
10. Negahban EO. Marlik: the complete excavation report, 2 vols. Philadelphia: University of Pennsylvania Museum of Archaeology and Anthropology, University of Pennsylvania; 1996.
11. Negahban EO. Excavation at Haft Tepe, Iran. Philadelphia: The University Museum of Archaeology and Anthropology, University of Pennsylvania; 1991.
12. Ghirshman R. Tchoga Zanbil (Dur-Untash) I. La ziggurat. Paris: MDAFI 39; 1966.
13. Fügert A, Gries H. 'I had baked bricks glazed in lapis lazuli color'-A Brief History of Glazed Bricks in the Ancient Near East. In: Fügert A, Gries H, editors. Glazed Brick Decoration in the Ancient Near East, Proceedings of a Workshop at the 11th International Congress of the Archaeology of the Ancient Near East, April 2018, Munich, Vorderasiatischesche Museum-Staatliche Museen zu Berlin, Oxford: Archaeopress; 2020. p. 1–15.
14. Yelon A, Saucier A, Larocque J, Smith P, Vandiver P. Thermal Analysis of Early Neolithic Pottery from Tepe Ganj Dareh, Iran. MRS Proc. 1992;267:591.
15. Marghussian AK, Coningham RAE, Fazeli H. The Evolution of Pottery Production During the Late Neolithic Period at Sialk On the Kashan Plain, Central Plateau of Iran. Archaeometry. 2017;59:222–38.
16. Marghussian AK, Fazeli H, Sarpoolaky H. Chemical–Mineralogical Analyses and Microstructural Studies of Prehistoric Pottery from Rahmatabad, South-West Iran. Archaeometry. 2009;51:733–47.

17. Meakes AA. Scientific Analysis of Neolithic Period Ceramics from Fars, Iran. PhD Thesis, University of Nottingham, 2016.
18. Fazeli H, Coningham RAE, Pollard AM. Chemical Characterisation of Late Neolithic and Chalcolithic Pottery from the Tehran Plain, Iran. Iran. 2001;39:55–71.
19. Emami M, Sakali Y, Pritzel C, Trettin R. Deep inside the ceramic texture: A microscopic–chemical approach to the phase transition via partial-sintering processes in ancient ceramic matrices. J Microsc Ultrastructure. 2016;4:11–9.
20. Kamilli DC, Lamberg-Karlovsky CC. Petrographic and electron microprobe analysis of ceramics from Tepe Yahya, Iran. Archaeometry. 1979;21:47–59.
21. Mutin B, Lamberg-Karlovsky CC, Minc L. Investigating ceramic production during the Proto-Elamite period at Tepe Yahya, southeastern Iran: Results of instrumental neutron activation analysis of periods IVC and IVB ceramics. J Archaeol Sci Rep. 2016;7:849–62.
22. Eslami M, Wicke D, Rajabi N. Geochemical analyses result of prehistoric pottery from the site of Tol-e Kamin (Fars, Iran) by pXRF. STAR: Science & Technology of Archaeological Research. 2020;6: 61–71.
23. Blackman MJ. The mineralogical and chemical analysis of Banesh period ceramics from Tal-e Malyan, Iran. In: Hughes MJ, editor. Scientific Stud Ancient Ceramics. London: British Museum Press; 1981. p. 7–20.
24. Sarhaddi-Dadiana H, Ramli Z, Abdul Rahman NHS, Mehrafarin RN. X-ray diffraction and X-ray fluorescence analysis of pottery shards from new archaeological survey in south region of Sistan, Iran. Mediterr Archaeol AR. 2015;15:45–56.
25. Eftekhari N, Holakooei P, Sayyadshahri H, Vaccaro C. Four shades of black: Non-invasive scientific studies on the painted potteries from Shahr-i Sokhta, Eastern Iran. J Archaeol Sci Rep. 2018;22:100–7.
26. Javanshah Z. Chemical and mineralogical analysis for Provenancing of the bronze age pottery from Shahr-i Sokhta, South Eastern Iran. Scientific Cult. 2018;4:83–92.
27. Stefanski A. Dynamics in ceramic production: petrographic analysis of ceramics from Godin Tepe III:6 and III:5, Iran. 2020; https://doi.org/10.1080/05786967.2020.1781545.
28. Heydarian M, Abdorrahimian F, Emami SMA, Beheshti SI. The provenance and distribution of early bronze ceramics in the Kolyaei Plain, Central Zagros, Iran, Archaeometry. 2020;62: 694–711.
29. Emami M, Trettin R. Mineralogical and chemical investigations on the ceramic technology in Čoǧā Zanbil, (Iran, 1250 B.C.). Period Mineral. 2012;81: 359–377.
30. Emami M, QXRD. XRF and optical microscopy applied to characterization and provenance of ancient ceramics from Haft Teppeh (1500 – 1150 BC), southwest Iran. IOP Conf Ser-Mat Sci. 2012;37:012012.
31. Heydarian M, Hajinorouzi F, Khosrowzadeh A, Beheshti SI, Emami M. Insight into the provenance and clustering of Middle Chalcolithic Ceramics from Chaharmahal-Bakhtiari, Iran: Using petrographic and ICP-OES analysis. J Archaeol Sci Rep. 2020;34:102655.
32. Oudbashi O, Naseri R, Malekzadeh K. Technical studies on the bronze age metal artefacts from the Graveyard of Deh Dumen, South-Western Iran (Third Millennium BC). Archaeometry. 2016;58:947–65.
33. Sołtysiak A, Naseri R, Najafi M. Human remains from Deh Dumen, Iran, 2019. Bioarchaeol Near East. 2019;13:142–6.
34. Sołtysiak A, Naseri R. Human remains from Deh Dumen, Iran, 2013–2016. Bioarchaeol Near East. 2017;11:70–5.
35. Anderson S. The Lizards of Iran, Society for the study of Amphibians and Reptiles. New York: Itacha; 1999.
36. Abyat Y, Abyat A, Abyat A. Microfacies and depositional environment of Asmari formation in the Zeloi oil field, Zagros basin, south-west Iran. Carbonate Evaporite. 2019;34:1583–93.
37. Allahkarampour Dill M, Seyrafian A, Vaziri-Moghaddam H. The Asmari Formation, north of the Gachsaran (Dill anticline), southwest Iran: Facies analysis, depositional environments and sequence stratigraphy. Carbonate Evaporite. 2010;25:145–60.
38. Eftekharifar R, Kharazian N, Parishani MR. Investigation of flora, life form and geographical distribution of plant species in north-west of Ludab region, Kohgiluyeh and Boyer-Ahmad province, Iran, Progress in Biological Sciences. 2017;7: 135–145.
39. Azadi A, Shakeri S. Effect of various land uses on potassium forms and some soil properties in Kohgiluyeh and Boyer-Ahmad Province, Southwest Iran. Iran Agricult Res. 2020;39:121–33.
40. Shakeri S, Abtahi SA. Potassium forms in calcareous soils as affected by clay minerals and soil development in Kohgiluyeh and Boyer-Ahmad Province, Southwest Iran. J Arid Land. 2018;10:217–32.
41. Owliaie HR. Micromorphology of pedogenic carbonate features in soils of Kohgilouye, Southwestern Iran. J Agr Sci Technol. 2012;14:225–39.
42. Owliaie HR, Abtahi A, Heck RJ. Pedogenesis and clay mineralogical investigation of soils formed on gypsiferous and calcareous materials, on a transect, Southwestern Iran. Geoderma. 2006;134:62–81.
43. Dehghanian MS, Khosrotehrani K, Afghah M, Keshani F. Microfacies Study of Asmari Formation in the Northwest and Southeast of Shiraz, Iran. Adv Environ Biol. 2012;6:556–63.
44. Roozpeykar A, Moghaddam IM. Biostratigraphy, facies analysis and paleoecology of the Asmari Formation in the northwest of Behbahan, south-western Iran. Carbonate Evaporite. 2015;30:387–400.
45. Martin JD. XPowder, XPowder12, XPowderXTM. In: A Software Package for Powder X-Ray Diffraction Analysis, Lgl. Dp. GR-780-2016; 2016.
46. Charola AE, Wendler E. An overview of the water-porous building materials interactions. Restoration Build Monuments. 2015;21:55–65.
47. - UNE-EN 13755. Métodos de ensayo para piedra natural. Determinación de la absorción de agua a presión atmosférica. Madrid: AENOR; 2008.
48. NORMAL 29/88. Misura dell'indice di asciugamento (drying index). Rome: ICR-CNR; 1988.
49. Cultrone G, de la Torre MJ, Sebastián E, Cazalla O. Evaluación de la durabilidad de ladrillos mediante técnicas destructivas (TD) y no-destructivas (TND). Mater Construcc. 2003;53:41–59.
50. RILEM. Recommended test to measure the deterioration of stone and to assess the differences of treatment methods. Mater Struct. 1980;13:175–253.
51. - Maniatis Y, Tite MS. Technological examination of Neolithic-Bronze Age pottery form central and Southeast Europe and from the near East. J Archaeol Sci. 1981;8:59–76.
52. Cultrone G, Carrillo Rosua FJ. Growth of metastable phases during brick firing: mineralogical and microtextural changes induced by the composition of the raw material and the presence of additives. Appl Clay Sci. 2020;185:105419.
53. Whitney DL, Evans BW. Abbreviations for names of rock-forming minerals. Am Mineral. 2010;95:185–7.
54. Rodriguez Navarro C, Cultrone G, Sanchez Navas A, Sebastian E. TEM study of mullite growth after muscovite breakdown. Am Mineral. 2003;88:713–24.
55. Peters T, Iberg R. Mineralogical changes during firing of calcium-rich brick clays. Ceramic Bull. 1978;57:503–9.
56. Sondi I, Juracic M. Whiting events and the formation of aragonite in the Mediterranean Karstic Marine Lakes: new evidence on its biologically induced organic origin. Sedimentology. 2010;57:85–95.
57. Macías Sánchez E, Willinger MG, Pina CM, Checa AG. Transformation of ACC into aragonite and the origin of the nanogranular structure of nacre. Sci Rep. 2017;7:12728.
58. Rodriguez Navarro C, Ruiz Agudo E, Luque A, Rodriguez Navarro AB, Ortega Huertas M. Thermal decomposition of calcite: mechanisms of formation and textural evolution of CaO nanocrystals. Am Mineral. 2009;94:578–93.
59. Cultrone G, Rodriguez Navarro C, Sebastian E, Cazalla O, de la Torre MJ. Carbonate and silicate phase reactions during ceramic firing. Eur J Mineral. 2001;13:621–34.
60. García Labiano F, Abad A, de Diego F, Gayán P, Adánez J. Calcination of calcium-based sorbents at pressure in a broad range of $CO_2$ concentrations. Chem Eng Sci. 2002;57:2381–93.
61. Maritan L, Nodari L, Mazzoli C, Milano A, Russo U. Influence of firing conditions on ceramic products: Experimental study on clay rich in organic matter. Appl Clay Sci. 2006;31:1–15.
62. Burke C, Day PM, Pullen DJ. The Cantribution of Petrography to Understanding the Production and Consumption of Early Hellenistic Ceramics from Nemea, Main land Greece. In: Ownby M, Druc I, Masucci M, editors. Investigative Approaches Ceramic Petrography. Salt Lake City: University of Utah Press; 2017.
63. Fabbri B, Gualtieri S, Shoval S. The presence of calcite in archaeological ceramics. J Eur Ceram Soc. 2014;34:1899–911.

64. Quinn PS. Ceramic petrography, the interdisciplinary of archaeological pottery & related artefacts in thin section. Oxford: Archaeopress; 2013.
65. - Reedy CL. Thin-section Petrography of Stone and Ceramic Cultural Materials. London: Archetype Publications; 2008.
66. Breakmans D, Degryse P. Petrography, Optical Microscopy. In: Hunt AMW, editor. The Oxford Handbook of Archaeological Ceramic Analysis. Oxford: Oxford University Press; 2017.
67. Whitbread IK. The characterization of argillaceous inclusions in ceramic thin sections. Archaeometry. 1986;28:79–88.
68. Brownell WE. Structural clay products. Vienna: Springer Verlag; 1976.
69. Molina E, Cultrone G, Sebastián E, Alonso FJ, Carrizo L, Gisbert J, Buj O. The pore system of sedimentary rocks as a key factor in the durability of building materials. Eng Geol. 2011;118:110–21.
70. Cultrone G, Sebastián E, Elert K, de la Totte MJ, Cazalla O, Rodriguez Navarro C. Influence of mineralogy and firing temperature on the porosity of bricks. J Eur Ceram Soc. 2004;24:547–64.
71. Pincé P, Braekmans D, Lycke S, Vandenabeele P. Ceramic Production in the Kur River Basin (Fars, Iran) During the Middle to Late Second Millennium BCE: A Geochemical and Technological Characterization. Archaeometry. 2019;61:556–73.
72. Marghussian AK. Reassessing the prehistoric ceramics of the Late Neolithic and Transitional Chalcolithic periods in the Central Plateau of Iran: Archaeometric Characterisation, Typological Classification and Stylistic Phylogenetic analyses, PhD Thesis, The Department of Archaeology, Durham University, 2017.
73. Nodari L, Maritan L, Mazzoli C, Russo U. Sandwich structures in the Etruscan-Padan type pottery. Appl Clay Sci. 2004;27:119–28.
74. Noghani S, Emami M. Mineralogical phase transition on sandwich-like structure of clinky pottery from parthian period, Iran. Period Mineral. 2014;83:171–85.
75. De Bonis A, Cultrone G, Grifa C, Langella A, Leone AP, Mercurio M, Morra V. Different shades of red: The complexity of mineralogical and physicochemical factors influencing the colour of ceramics. Ceram Int. 2017;43:8065–74.
76. Colomban P, Ngoc Khoi D, Quang Liem N, Roche C, Sagon G. Sa Huynh and Cham potteries: microstructure and likely processing. J Cult Herit. 2004;5:149–55.
77. Levin EM, Robbins CR, McMurdie HF, Reser MK. Phase Diagrams for Ceramists, Colombus: The American Ceramic Society, 1964.
78. Lahlil S, Bouquillon A, Morin G, Galoisy L, Lorre C. Relationship between the coloration and the firing technology used to produce Susa Glazed ceramics of the end of the Neolithic Period. Archaeometry. 2009;51:774–90.
79. Begemann F, Haerinck E, Overlaet B, Schmitt-Strecker S, Tallon F. An Archaeo-Metallurgical Study of the Early and Middle Bronze Age in Luristan, Iran, Iran Antiq. 2008;XLIII: 2–66.
80. Haerinck E, Overlaet B. Luristan Excavation Documents Vol. VII: The Kalleh Nisar Bronze Age Graveyard in Pusht-i Kuh, Luristan, Acta Iranica 46, Leuven: Peeters Publishers; 2008.
81. Haerinck E, Overlaet B, Luristan Excavation Documents VI. Bani Surmah: An Early Bronze Age Graveyard in Pusht-i Kuh, Luristan, Acta Iranica, 43. Leuven: Peeters Publishers; 2006.
82. Potts DT. Luristan and the Central Zagros in the Bronze Age. In: Potts DT, editor. The Oxford Handbook of Ancient Iran. Oxford: Oxford University Press; 2013. p. 203–17.
83. Mohammadi Z, Raeisi E, Bakalowicz M. Evidence of karst from behaviour of the Asmari limestone aquifer at the Khersan 3 Dam site, southern Iran. Hydrolog Sci J. 2007;52:206–20.
84. Stocklin J. Structural history and tectonics map of Iran: a review. AAPG Bull. 1968;52:1229–58.
85. James GA, Wynd JG. Stratigraphic nomenclature of Iranian oil consortium agreement area. AAPG Bull. 1965;49:2182–245.


## Publisher's Note